Theoretical Analysis of Dental Demineralization using Photothermal Radiometry

A. Mandelis[a,b], A. Matvienko[a,b], S.H. Abrams[b]

[a]Center for Advanced Diffusion Wave Technologies, Department of Mechanical and Industrial Engineering, University of Toronto, 5 King's College Road, Toronto, Ontario, M5S 3G8, Canada;
[b]Quantum Dental Technologies, 748 Briar Hill Avenue, Toronto, Ontario, M6B 1L3, Canada.

ABSTRACT

A coupled diffuse-photon-density-wave and thermal-wave theoretical model was developed to describe the biothermophotonic phenomena in a turbid medium under photothermal radiometry experimental conditions. The solution of the radiative transport equation in the limit of the diffuse-photon-density field was considered as a source term in the thermal-wave field equation. The model was used to analyze laser induced photothermal phenomena in a demineralized tooth sample as a function of depth. The analysis is based on a three-layer approach (demineralized enamel + healthy enamel + dentin) and considering the influence of thermal and optical properties of each layer on the resulting optical and thermal field.

Keywords: Photothermal, biothermophotonic, dental, optical properties, thermal properties

1. INTRODUCTION

Numerous studies have been focused on the *in vivo* evaluation of optical properties of biological tissues. In many cases, these results are based on the radiative transport theory with various modifications (particularly, the diffusion approximation)[1] depending on the applied measurement technique. The main restriction to applications of the diffusion theory is that scattering effects must be significant, which is, however, commonly the case with tissues. In particular, the requirement of mean-free-path for photon scattering being much larger than the wavelength of light and much smaller then the thickness of the medium allows the description of multiply scattered light intensity by means of diffusion equation.[2] Additional constrains are related to the size of the scattering particles, which should be small compared to the optical wavelength.[2]

Another model used for calculations of optical properties from experimental results is the Monte Carlo approach, which describes pathways of photons in the material on a random basis.[3] This method can be applied to samples with any absorption-to-scattering coefficient ratio, but the long time required for calculations restricts its efficiency. The method involves an iterative procedure of adjustment of calculated optical properties according to the Monte Carlo modeled predictions for the data on diffuse or collimated reflectance and transmittance.

During the past decade, coupled-field (photoacoustic and photothermal) techniques attracted much attention since the secondary (acoustic or thermal) signal detection can significantly increase resolution of pure optical characterization. Moreover, they allow comprehensive and simultaneous analysis of optical and thermal properties of tissue during laser irradiation. The photoacoustic methods are based on the study of laser-induced stress transient (optoacoustic or photoacoustic),[4,5] while photothermal techniques concern laser-induced thermal field in a sample. The most common photothermal method applied to biological tissue investigations is photothermal radiometry (PTR). Two major types of PTR applications to tissue analysis are described in literature: pulsed photothermal radiometry,[6-8] and frequency-domain photothermal radiometry.[9-11] These methods have distinct advantages for biomedical imaging and diagnosis due to their non-invasive character.

*mandelis@mie.utoronto.ca

Pulsed (or frequency-domain) radiometry methods are based on the thermal infrared response of a medium to a single-pulse (or frequency-modulated) laser irradiation following optical-to-thermal energy conversion. The generated signals carry subsurface information in the form of a temperature depth integral, allowing analysis of the medium well below the range of optical imaging. Based on the measured infrared signal, both optical and thermal characteristics of tissues can be evaluated non-invasively. Pulsed photothermal radiometry was applied to various tissue measurements, including dental enamel.[12,13] However, the temporal decay of the thermal pulse represents only one signal channel available to analysis, requiring an additional independent optical measurement to extract a reliable set of optical parameters.[7]

Frequency-domain photothermal radiometry provides two signal channels (amplitude and phase). In this method, a harmonically modulated laser beam generates diffuse-photon-density waves in a turbid medium. Following photon migration (diffusion) and scattering, the absorbed fraction of the diffusive light creates an oscillatory temperature (thermal-wave) field, which is detected radiometrically.

The complete theoretical formalism of photothermal radiometry includes the description of two fields: optical and thermal. For pulsed photothermal radiometry, a coupled analysis of these fields has been introduced.[7] The authors considered the one-dimensional diffusion approximation for the absorbing and scattering optical fields and the Green function approach for the heat conduction equation in a homogeneous turbid medium. The model was applied for the measurements of optical properties of samples, while the thermal properties were known. A similar analysis for the simpler case of only absorbing (but not scattering) tissue has been applied to the thermal diffusivity evaluation of skin with known optical properties.[14] These studies demonstrated the important potential of photothermal radiometry as a novel tool for in-vivo thermal analysis of tissues, which is traditionally done with invasive methods such as measurements of thermal response with a set of sensor probes inserted into tissues.

A theoretical approach for the application of frequency domain photothermal radiometry for non-invasive simultaneous optical and thermal characterization of turbid media has recently been introduced.[15,16] The authors developed a rigorous three-dimensional model for frequency-domain photothermal radiometry of a single-layer tissue, where the diffuse-photon-density field in the laser-irradiated tissue acts as a modulated source for the thermal-wave field. This method was later applied for the optical and thermal evaluation of dental enamel.[11] However, in many cases biological tissues are not homogeneous. For example, a demineralized tooth has a layered structure: demineralized enamel, intact enamel, dentin, and pulp. There are a number of studies on the optical evaluation of layered media.[17-19]

To our best knowledge, there have been no attempts in literature to describe coupled diffuse-photon-density wave and thermal-wave fields for the photothermal radiometric analysis of layered tissues. In this paper, we expand the theoretical formalism developed for the frequency-domain photothermal radiometry of a single-layer turbid medium to the three-layer case and show the capabilities of the model to describe diffuse-photon-density and thermal-wave profiles as functions of the layer properties. The motivation for these studies is the assessment of the capabilities of photothermal radiometry to monitor quantitatively the demineralization of dental enamel by acidic agents contained in food and drinks as well as through the action of bacteria.

2. THEORETICAL MODEL

We assume that a tooth has a three-layered one-dimensional turbid structure and irradiated with laser light (Fig 1). As a result of the incident radiation, a one-dimensional total photon field Ψ_t arises inside the medium. It can be divided into two components:

$$\Psi_{t_i}(z;\omega) = \Psi_{c_i}(z;\omega) + \Psi_{d_i}(z;\omega) \tag{1}$$

where Ψ_c is the coherent photon density and Ψ_d is the diffuse photon density of the turbid medium. Here, the subscript i denotes 1 – demineralized layer, 2 – intact enamel, 3 – dentin.
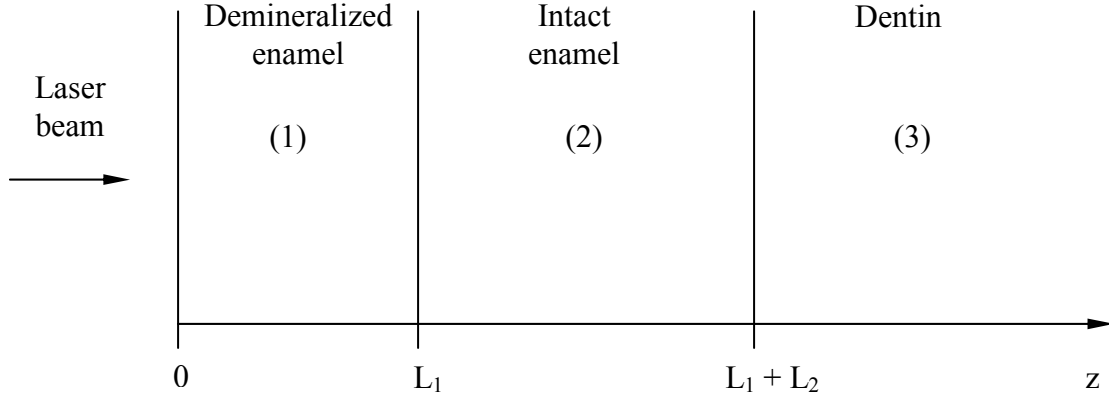
Figure 1. Three-layer one-dimensional model of a demineralized tooth section.

The analysis of depth profiles of the optical and thermal fields in hard dental tissue (see Section III) shows that meaningful change in the temperature field occurs only up to the certain depth, which in dental tissue is usually less than 3-4 mm. The thickness of human dental enamel varies from 0.8 to 1.95 mm[20] and the dentin thickness varies from about 4 to 9 mm.[21] In practice, the combined layer would definitely be thicker than 3-4 mm, therefore the model doesn't involve the pulp layer, which is too deep to matter.

The one-dimensional coherent photon-density field takes into account the reduction of the incident intensity due to scattering and absorption:

$$\Psi_{c_1} = I_0 \left(1-R\right) \exp\left(-\mu_{t_1} z\right)$$
$$\Psi_{c_2} = I_0 \left(1-R\right) \exp\left(-\mu_{t_1} L_1\right) \exp\left[-\mu_{t_2}\left(z-L_1\right)\right] \quad (2)$$
$$\Psi_{c_3} = I_0 \left(1-R\right) \exp\left[-\left(\mu_{t_1} L_1 + \mu_{t_2} L_2\right)\right] \exp\left\{-\mu_{t_3}\left[z-\left(L_1+L_2\right)\right]\right\}$$

where I_0 is the laser intensity, R is the reflectivity of the outermost turbid medium (enamel), and

$$\mu_{t_i} = \mu_{a_i} + \mu_{s_i} \quad (3)$$

Here, μ_t is the total attenuation coefficient of layer i, which includes absorption coefficient μ_z, [m⁻¹], and scattering coefficient μ_s, [m⁻¹], of the medium.

The one-dimensional diffuse-photon-density equation in frequency domain can be described as:[15]

$$\frac{d^2}{dz^2}\Psi_{d_i}\left(z\right) - 3\mu_{a_i}\mu'_{t_i}\Psi_{d_i}\left(z\right) = -\frac{1}{D_i}G_i\left(z\right), \quad i=1,2,3. \quad (4)$$

Here, the optical diffusion coefficient, which represents the mean free path of photons limited by absorption and scattering is defined as:[22]

$$D = 1/3\mu_t' \quad (5)$$

with the reduced attenuation coefficient:

$$\mu_t' = \mu_a + \left(1-g\right)\mu_s \quad (6)$$

where g is the mean cosine of the scattering angle. For tissues, the reduced attenuation coefficient, Eq. (6), is much smaller than the total attenuation coefficient, Eq. (3), due to a high value of the mean cosine of the scattering angle g, which is close to unity for highly scattering turbid media.[1]

The function $G(z)$ represents a photon source and depends on the optical properties of medium.[15] In the case of diffusion-photon-wave propagation in tissues, the typical value of the inverse diffuse-photon absorption where the function G_i is equal to:

$$G_i(z) = \mu_{s_i} \left(\frac{\mu_{t_i} + g_i \mu_{a_i}}{\mu_{t_i} - g \mu_{s_i}} \right) \Psi_{c_i} \tag{7}$$

The general solutions for the optical fields for each layer ($i = 1,2,3$), including coherent and diffuse components, can be written as:

$$\begin{aligned}
\Psi_{t_1}(z) &= a_1 \exp(Q_1 z) + b_1 \exp(-Q_1 z) + \left[d_1 + (1-R) I_0 \right] \exp\left(-\mu_{t_1} z\right) \\
\Psi_{t_2}(z) &= a_2 \exp\left[Q_2(z - L_1) \right] + b_2 \exp\left[-Q_2(z - L_1) \right] \\
&\quad + \left[d_2 + (1-R) I_0 \exp\left(-\mu_{t_1} L_1\right) \right] \exp\left[-\mu_{t_2}(z - L_1) \right] \\
\Psi_{t_3}(z) &= b_3 \exp\left\{ -Q_3 \left[z - (L_1 + L_2) \right] \right\} \\
&\quad + \left[d_3 + (1-R) I_0 \exp\left(-\mu_{t_1} L_1\right) \exp\left(-\mu_{t_2} L_2\right) \right] \exp\left\{ -\mu_{t_3} \left[z - (L_1 + L_2) \right] \right\}
\end{aligned} \tag{7}$$

where the integration constants d_1-d_3 are due to the coherent field solutions.

It should be mentioned here, that for the case of dentin, the dc photon diffusion depth:[22]

$$\sqrt{D/\mu_a} = \sqrt{1/\left(3\mu_a \mu'_t\right)} \tag{8}$$

is about 0.6 μm (literature values for the properties of dental tissues are listed in Table I), which is much less than the dentin layer thickness. Therefore, a semi-infinite assumption will be valid for the dentin layer in Eq. (7). This consideration further justifies the modeling of human teeth as three-layer photothermal structures.

The boundary conditions applied in the study are of the so-called "third-kind" at the air-tooth interface, as well as continuity of photon-density field and photon flux at the interfaces between solid layers. The detailed solution of the system is presented in our recent study.[23]

The total diffuse photon density field Ψ_t is a source of the much more slowly propagating thermal-wave field given by:

$$\frac{d^2}{dz^2} T_i(z; \omega) - \sigma_i^2 T_i(z; \omega) = -\eta_{NR} \frac{\mu_{a_i}}{\kappa_i} \Psi_{t_i}(z; \omega); \quad i = 1, 2, 3 \tag{9}$$

where

$$\sigma_i = \sqrt{\frac{i\omega}{\alpha_i}} \tag{10}$$

is the thermal-wave number, [m^{-1}], which depends on the modulation frequency and thermal diffusivity α, [m^2/s], of i-th layer. Here, η_{NR} is non-radiative efficiency and κ is the thermal conductivity of the i-th layer, [W/mK].

Taking into account the semi-infinite character of the dentin layer, the thermal-wave fields for each layer can be written in the form:

$$T_1(z;\omega) = A_1 \exp(\sigma_1 z) + B_1 \exp(-\sigma_1 z) + C_1 \exp(Q_1 z) + D_1 \exp(-Q_1 z) + E_1 \exp(-\mu_{t_1} z);$$

$$T_2(z;\omega) = A_2 \exp\left[\sigma_2(z-L_1)\right] + B_2 \exp\left[-\sigma_2(z-L_1)\right] + C_2 \exp\left[Q_2(z-L_1)\right]$$
$$+ D_2 \exp\left[-Q_2(z-L_1)\right] + E_2 \exp\left[-\mu_{t_2}(z-L_1)\right]; \tag{11}$$

$$T_3(z;\omega) = B_3 \exp\left\{-\sigma_3\left[z-(L_1+L_2)\right]\right\} + D_3 \exp\left\{-Q_3\left[z-(L_1+L_2)\right]\right\}$$
$$+ E_3 \exp\left\{-\mu_{t_3}\left[z-(L_1+L_2)\right]\right\};$$

Again, the dentin layer is considered semi-infinite, since the thermal diffusion depth,

$$\sqrt{2\alpha_3/\omega}, \tag{12}$$

for example at 1 Hz, is equal to 0.29 mm (dentin properties are listed in Table I), which is much less than the dentin thickness. The solution of the problem in detail is discussed on our recent study.[23]

3. DIFFUSE-PHOTON AND THERMAL-WAVE FIELD SIMULATIONS

Theoretical simulations of the total diffuse-photon field, Eq. (7), and the thermal-wave field, Eq. (11), were performed to show the influence of thermal and optical parameters of the dental tissue layers (Table I) on the field distributions. It is obvious from the mathematical structure of Eqs. (7) and (11) that some tissue properties have a stronger impact on the photon and thermal-wave propagation through the media than others. Identifying those groups of parameters will help strengthen multi-parameter analysis by fixing some variables which do not affect the field distribution significantly, thus reducing the degrees of freedom in the fitting procedure of experimental data.

While the thermal-wave field is both coordinate and frequency dependent, the diffuse-photon field is inherently a dc field in the frequency range of our experiments and is only spatially distributed. Since thermal properties do not influence photon propagation in the narrow temperature range of our experiments, the diffuse-photon-field analysis is further reduced to the demonstration of the role of optical parameters of the various layers in the resulting photon field distribution.

Table I. Optical (632 nm) and thermal properties of dental tissues[24-26]

	Optical absorption coefficient μ_a, m^{-1}	Optical scattering coefficient μ_s, m^{-1}	Thermal diffusivity α, m^2/s	Thermal conductivity κ, W/mK
Enamel	<100	6000±1800	(4.2 - 4.69)·10-7	0.913-0.926
Dentin	300-400	28000±8400	(1.87 – 2.6)·10-7	0.577-0.623

Figure 2 shows the depth profile of the diffuse-photon and thermal-wave fields for various absorption coefficients of the demineralized enamel layer. The diffuse-photon density decays over the depth of the sample. That is clearly seen from the comparison of the curves in the enamel (z < 0.8 mm) and dentin (z > 0.8 mm) regions. The assumed absorption coefficient of dentin is 400 m^{-1}, which is higher than the absorption coefficients considered for both demineralized and healthy enamel (Table I), so the absorption process is more efficient in the dentin, and the density of available photons decreases here more rapidly as a function of depth. For the very same reason, photon density decreases with increasing value of the absorption coefficient at a fixed depth due to the enhanced de-excitation rate.

The corresponding thermal-wave amplitude, Fig. 2, does not decrease monotonically over the sample depth. The amplitude exhibits a local maximum at the enamel-dentin interface, since higher absorption in dentin creates a stronger thermal-wave field, as more photons are converted into heat, but they are on the other side of the enamel layer and

generate an exponentially decreasing thermal-wave field. The amplitude decreases in the dentin region as less optical power is transmitted into the medium. At a fixed demineralized enamel depth the amplitude is higher for larger absorption coefficients, since the field source is stronger. At the same time, fewer photons are transmitted farther, so the amplitude decreases more rapidly for higher absorption coefficients, which, however, appears on a logarithmic scale as a constant offset between the three decreasing curves at deeper regions.

The thermal-wave phase is more sensitive to the change in absorption coefficient, so the phase lag is smaller for the medium with higher absorption coefficient and a crossover behavior, consistent with the changes in the amplitude, is obvious. The oscillatory phase shift represents the formation of a standing thermal wave. An increase in the absorption coefficient confines the sub-surface extent of the thermal wave to a narrower region which enhances the interference between forward propagating and interface-interacted thermal waves,[27] resulting in stronger peak-to-peak phase interferometric patterns. As expected, the higher absorption coefficient (200 m^{-1}) leads to the smaller phase lag, and it increases more steeply from the demineralized region into the healthy enamel than those associated with lower absorption cases, since photons are absorbed at a higher spatial rate generating a steeper thermal-wave gradient.
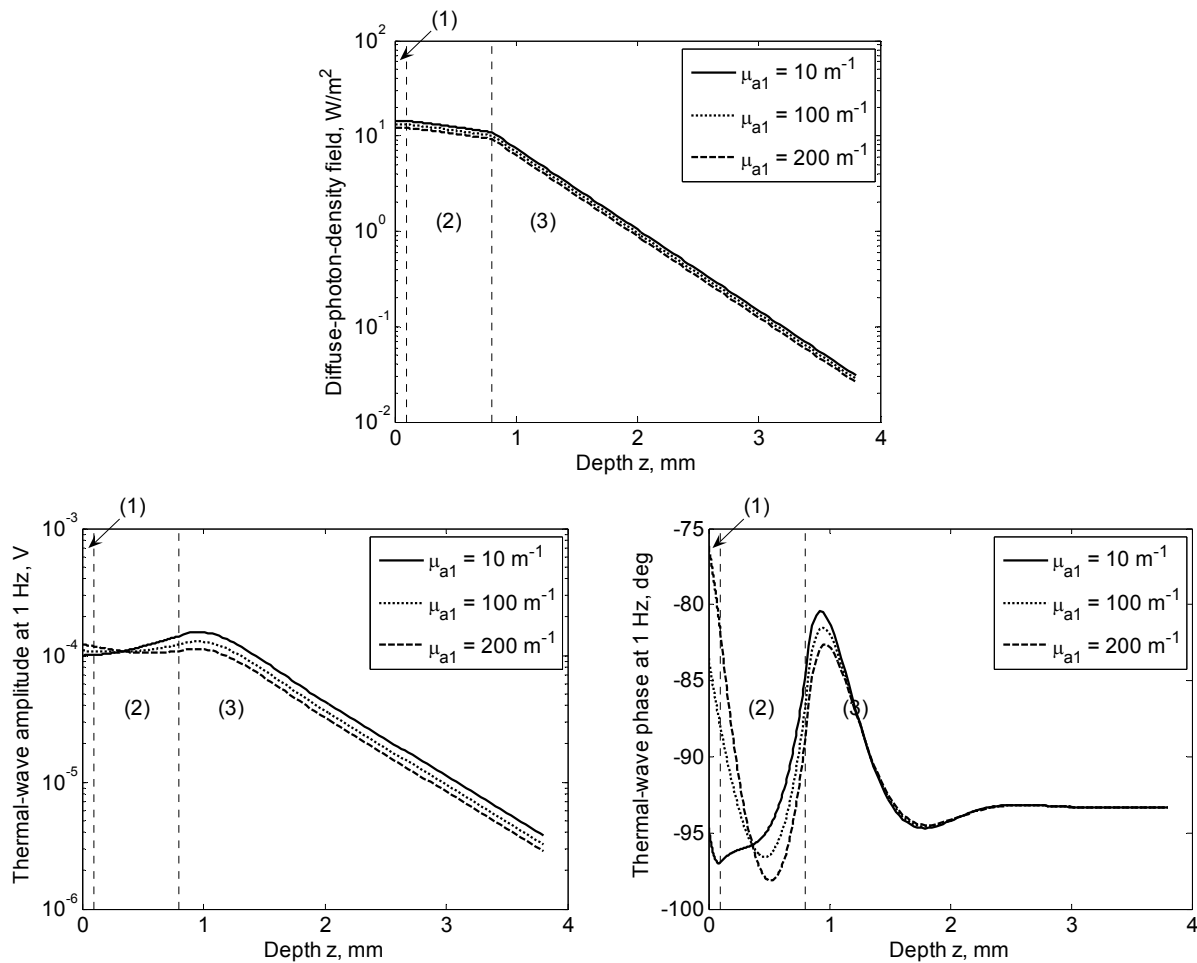

Figure 2. Photon and thermal-wave field depth distribution in a layered tooth sample: variation in absorption coefficient of demineralized enamel. The assumed values of parameters are: $\mu_{a2} = 100$ m^{-1}, $\mu_{a3} = 400$ m^{-1}, $\mu_{s1} = 6000$ m^{-1}, $\mu_{s2} = 6000$ m^{-1}, $\mu_{s3} = 28000$ m^{-1}, $\alpha_1 = 5\times10^{-7}$ m^2/s; $\alpha_2 = 5\times10^{-7}$ m^2/s, $\alpha_3 = 2\times10^{-7}$ m^2/s, $\kappa_1 = 0.9$ W/mK, $\kappa_2 = 0.9$ W/mK, $\kappa_3 = 0.6$ W/mK, $\eta_{NR1} = 0.5$, $\eta_{NR2} = 0.5$, $\eta_{NR3} = 0.5$, $\mu_{IR} = 100000$ m^{-1}, $L_1 = 100$ µm, $L_2 = 700$ µm, $L_3 = 3000$ µm.

Similar trends in the behavior of optical and thermal fields were observed with the variation of absorption coefficient of other layers.[23] It was also found that scattering coefficient does not significantly influence the optical and thermal-wave profiles.[23]

Another interesting aspect of the thermal-wave field propagation is the influence of the thermophysical parameters of turbid media. Figure 3 represents the example of the variation in the thermal diffusivity of the demineralized enamel and corresponding changes in the depth profiles of the thermal-wave field. Unlike homogeneous and opaque solids, the depth profile of the thermal-wave amplitude exhibits an increase with increasing thermal diffusivity of the demineralized layer. This increase is caused by the fact that the sub-surface thermal-wave sources in layers (2) and (3) can contribute more efficiently to heat diffusion from bulk to surface and raise the thermal-wave amplitude with increased α_1. The thermal-wave phase lag for larger thermal diffusivity, Fig. 3, is smaller at $z = 0$ and nearby depths due to the enhanced back-propagated thermal-wave diffusion from sub-surface absorptions, so that the thermal-wave centroid shifts closer to the surface. Similar behavior was observed for the change in the thermal diffusivity of intact enamel and dentin layers.[23]
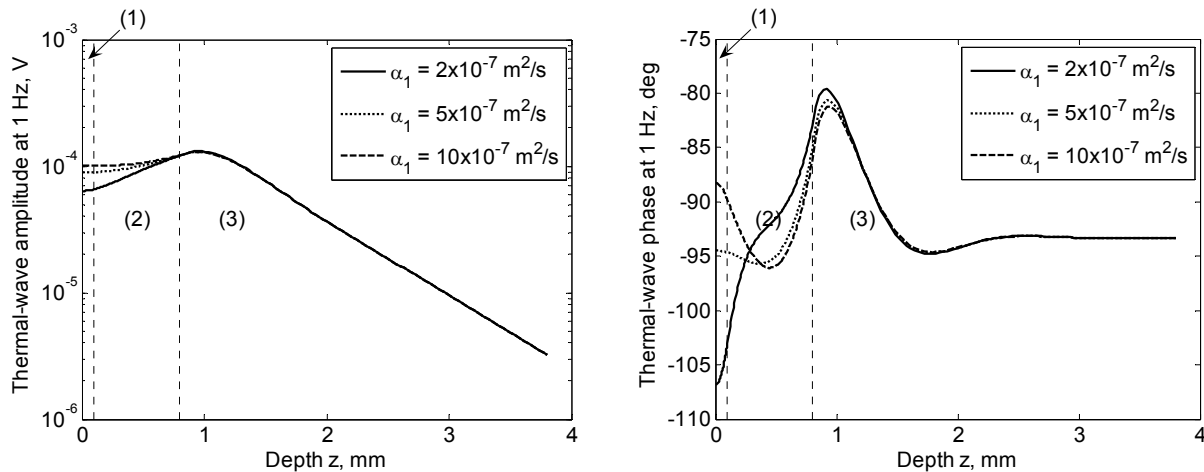

Fig. 3. Thermal-wave field depth distribution in a layered tooth sample: variation in thermal diffusivity of demineralized enamel. The assumed values of parameters are: $\mu_{a1} = 100$ m^{-1}, $\mu_{a2} = 100$ m^{-1}, $\mu_{a3} = 400$ m^{-1}, $\mu_{s1} = 6000$ m^{-1}, $\mu_{s2} = 6000$ m^{-1}, $\mu_{s3} = 28000$ m^{-1}, $\alpha_2 = 5 \times 10^{-7}$ m^2/s; $\alpha_3 = 2 \times 10^{-7}$ m^2/s, $\kappa_1 = 0.9$ W/mK, $\kappa_2 = 0.9$ W/mK, $\kappa_3 = 0.6$ W/mK, $\eta_{NR1} = 0.5$, $\eta_{NR2} = 0.5$, $\eta_{NR3} = 0.5$, $\mu_{IR} = 100000$ m^{-1}, $L_1 = 100$ µm, $L_2 = 700$ µm, $L_3 = 3000$ µm.
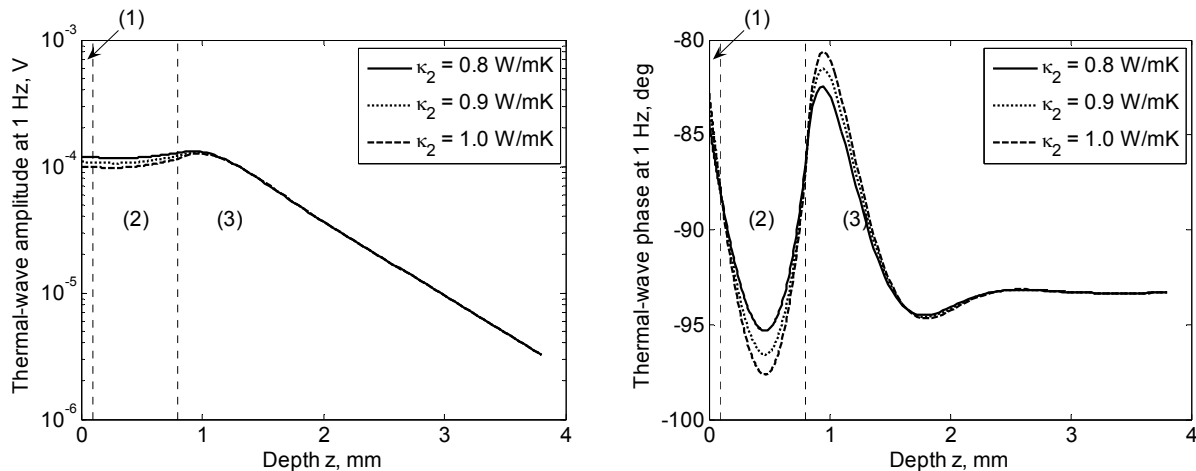

Fig. 4. Thermal-wave field depth distribution in a layered tooth sample: variation in thermal conductivity of intact enamel. The assumed values of parameters are: $\mu_{a1} = 100$ m^{-1}, $\mu_{a2} = 100$ m^{-1}, $\mu_{a3} = 400$ m^{-1}, $\mu_{s1} = 6000$ m^{-1}, $\mu_{s2} = 6000$ m^{-1}, $\mu_{s3} = 28000$ m^{-1}, $\alpha_1 = 5 \times 10^{-7}$ m^2/s; $\alpha_2 = 5 \times 10^{-7}$ m^2/s; $\alpha_3 = 2 \times 10^{-7}$ m^2/s, $\kappa_1 = 0.9$ W/mK, $\kappa_3 = 0.6$ W/mK, $\eta_{NR1} = 0.5$, $\eta_{NR2} = 0.5$, $\eta_{NR3} = 0.5$, $\mu_{IR} = 100000$ m^{-1}, $L_1 = 100$ µm, $L_2 = 700$ µm, $L_3 = 3000$ µm.

The change in the thermal conductivity of the demineralized layer did not visibly affect the thermal-wave field due to its small thickness.[23] However, with the conductivity variation in the thicker healthy enamel, depth profile changes are more prominent (Fig. 4). For lower thermal conductivity, less thermal-wave power is transported forward into the layered structure under the optically imposed thermal-wave gradient, so the thermal-wave amplitude is somewhat larger in this case. The increase in thermal conductivity facilitates thermal energy propagation and L_2 interference between forward and interface-interacted (back-propagating) thermal waves. Therefore, the strength of the thermal-wave phase oscillations increases. Similar trends were observed for the thermal conductivity variations in dentin.[23]

In conclusion, the developed theoretical model for the coupled diffuse-photon-density-wave and thermal-wave field can adequately explain photothermal phenomena in a layered tissue structure during modulated laser irradiation. The model will be further used for the fitting of the experimental data on the photothermal radiometry of demineralized teeth in order to extract thermal and optical parameters of the layers. This will allow characterization of the properties of demineralized layers and their differentiation from healthy enamel, thus leading to the quantitative detection of dental demineralization.

REFERENCES

[1]   A. Ishimaru, "Diffusion of light in turbid material," Appl. Opt. **28**, 2210-2215 (1989).

[2]   A. Ishimaru, Y. Kuga, R.L.T. Cheung, K. Shimizu, "Scattering and diffusion of beam wave in randomly distributed scatterers," J. Opt. Soc. Am. **73**, 131-136 (1983).

[3]   E.D. Cashwell, C.J. Everett, *Monte Carlo Method for Random Walk Problems*, Pergamon, London, 1959.

[4]   A.A. Oraevsky, S.L. Jaques, F.K. Tittel, "Measurement of tissue optical properties by time-resolved detection of laser-induced transient stress," Appl. Opt. **36**, 402-415 (1997).

[5]   P.S. Grashin, A.A. Karabutov, A.A. Oraevsky, I.M. Pelivanov, N.V. Podymova, E.V. Savateeva, V.S. Solomatin, "Distribution of the laser radiation intensity in turbid media: Monte Carlo simulations, theoretical analysis, and results of optoacoustic measurements," Quantum Electron. **32**, 868-874 (2002).

[6]   R.R. Anderson, H. Beck, U. Bruggemann, W. Farinelli, S.L. Jaques, J.A. Parrish, "Pulsed photothermal radiometry in turbid media: internal reflection of backscattered radiation strongly influences optical dosimetry," Appl. Opt. **28**, 2256-2262 (1989).

[7]   S.A. Prahl, I.A. Vitkin, U. Bruggemann, B.C. Wilson, R.R. Anderson, "Determination of optical properties of turbid media using pulsed photothermal radiometry," Phys. Med. Biol. **37**, 1203-1217 (1992).

[8]   S.L. Jaques, J.S. Nelson, W.H. Wright, T.E. Milner, "Pulsed photothermal radiometry of port-wine-stain lesions," Appl. Opt. **32**, 2439-2446 (1993).

[9]   L.O. Svaasand, B.J. Tromberg, R.C. Haskell, T.T. Tsay, M.V. Berns, "Tissue characterization and imaging using photon density waves," Opt. Eng. **32**, 313-321 (1993).

[10]   L. Nicolaides, A. Mandelis, S.H. Abrams, "Novel dental dynamic depth profilometric imaging using simultaneous frequency-domain infrared photothermal radiometry and laser luminescence," J. Biomed. Opt. **5**, 31-39 (2000).

[11]   L. Nicolaides, C. Feng, A. Mandelis, S.H. Abrams, "Quantitative dental measurements by use of simultaneous frequency-domain laser infrared photothermal radiometry and luminescence," Appl. Opt. **41**, 768-777 (2002).

[12]   D. Fried, W. Seka, R.E. Glena, J.D.B. Featherstone, "Thermal response of hard dental tissues to 9- through 11-mu m CO_2-laser irradiation," Opt. Eng. **35**, 1976-1984 (1996).

[13]   M.J. Zuerlin, D. Fried, J.D.B. Featherstone, W. Seka, "Optical properties of dental enamel in the mid-IR determined by pulsed photothermal radiometry," IEEE J. Quantum Electron. **5**, 1083-1089 (1999).

[14]   S.A. Telenkov, J.I. Youn, D.M. Goodman, A.J. Welch, T.E. Milner, "Non-contact measurement of thermal diffusivity in tissue," Phys. Med. Biol. 46 (2001) 551-558.

[15]   A. Mandelis, C. Feng, "Frequency-domain theory of laser infrared photothermal radiometric detection of thermal waves generated by diffuse-photon-density wave fields in turbid media," Phys. Rev. E **65**, 021909 (2002).

[16]   L. Nicolaides, Y. Chen, A. Mandelis, I.A. Vitkin, "Theoretical, experimental, and computational aspects of optical property determination of turbid media by using frequency-domain laser photothermal radiometry," J. Opt. Soc. Am. A **18**, 2548-2556 (2001).

[17]   J.M. Schmitt, G.X. Zhou, E.C. Walker, R.T. Wall, "Multilayer model of photon diffusion in skin," J. Opt. Soc. Am. A **7**, 2141-2153 (1990).

[18]   L.O. Svaasand, T. Spott, J.B. Fishkin, T. Pham, B.J. Tromberg, M.W. Berns, "Reflectance measurements of layered media with diffuse photon-density waves: a potential tool for evaluating deep burns and subcutaneous lesions," Phys. Med. Biol. **44**, 801-813(1999).

[19]   A. Kienle, M.S. Patterson, N. Dognitz, R. Bays, G. Wagnieres, H. van den Bergh, "Noninvasive determination of the optical properties of two-layered turbid media," Appl. Opt. **37**, 779-791 (1998).

[20]   T.M. Smith, A.J. Olejniczak, D.J. Reid, R.J. Ferrell, J.J. Hublin, "Modern human molar enamel thickness and enamel-dentine junction shape," Arch. Oral Biol. **51**, 974-995 (2006).

[21]   J.L. Stroud, P.H. Buschang, P.W. Goaz, "Sexual dimorphism in mesiodistal dentin and enamel thickness, " Dentomaxillofacial Radiology **23**, 169-171 (1994).

[22]   A. Mandelis, *Diffusion-Wave Fields: Mathematical Methods and Green Functions*, Springer, New York, 2001.

[23]   A. Matvienko, A. Mandelis, R.J. Jeon, S.H. Abrams, "Theoretical analysis of coupled diffuse photon density and thermal-wave field depth profiles photothermally generated in layered turbid dental structures," Phys. Rev. E, to be submitted.

[24]   D.Fried, R.E. Glena, J.D.B. Featherstone, W. Seka, "Nature of light scattering in dental enamel and dentin at visible and near-infrared wavelengths," Appl. Opt. **34**, 1278-1285 (1995).

[25]   W.S. Brown, W.A. Dewey, H.R. Jacobs, "Thermal properties of teeth," J. Dent. Res. **49**, 752 (1970).

[26]   M. Braden, "Heat conduction in normal human teeth," Arch. Oral Biol. **9**, 479-486 (1964).

[27]   A. Mandelis, L. Nicolaides, Y. Chen, "Structure and the reflectionless/refractionless nature of parabolic diffusion-wave fields," Phys. Rev. Lett. **87**, 020801(2001).